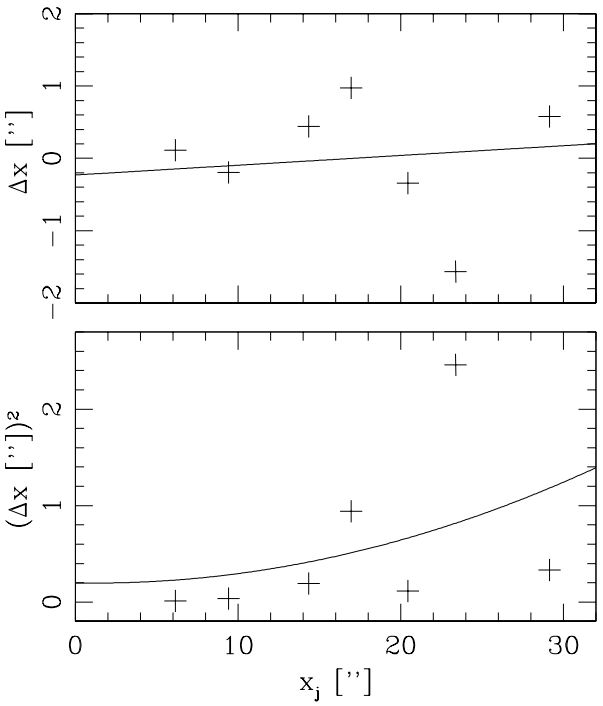

Fig. 1. Model fit to the HH 34 jet/counterjet knot pairs. We take the positions of the knots within 30″ from the outflow source (from Raga et al. 2011) and plot $\Delta x = x_j - x_{cj}$ (the jet/counterjet knot position offset, top graph) and $(\Delta x)^2$ (bottom graph) as a function of x_j. The straight line in the top graph and the curve in the bottom graph show the model fits, which result in the parameters given in Table 1.

nearly one third of the standard ∼2″ IRAC angular resolution.

As described in Raga et al. (2011) and Noriega-Crespo et al. (2011), given the collisional excitation characteristics of young stellar outflows like HH 34 and 111, the emission in the IRAC bandpasses is likely to be dominated by the pure rotational H_2 lines (e.g., Noriega-Crespo et al. 2004a,b; Looney, Tobin & Kwon 2007; Tobin et al. 2007; Ybarra & Lada 2009; De Buizer & Vacca 2010). Finally, in the HH 111 image we carried out astrometry of several field stars in order to correctly locate the position of the VLA 1 source (the source of the HH 111 outflow, see, e.g., Rodríguez et al. 2008).

3.3. *The HH 34 knots*

For the HH 34 outflow, we consider the 7 quasi-symmetric knot pairs detected in the *Spitzer* image of Raga et al. (2011). These knots lie at angular distances <30″ from the source, and have a clear correspondence between the jet and the counterjet.

TABLE 1

FITS TO THE HH 34/111 KNOTS

	HH 34	HH 111
a_1	$(-0.23 \pm 0.72)''$	$(2.19 \pm 0.85)''$
b_1	0.024 ± 0.039	0.027 ± 0.011
a_2	$(0.20 \pm 0.48)['']^2$	$(8.5 \pm 4.1)['']^2$
c_2	$(1.26 \pm 1.10) \times 10^{-3}$	$(0.93 \pm 0.42) \times 10^{-3}$
v_j	150 km s^{-1}	240 km s^{-1}
τ_0	(-3.0 ± 9.5) yr	(18.1 ± 7.0) yr
v_0	(2.0 ± 5.9) km s^{-1}	(6.5 ± 2.6) km s^{-1}
$\Delta\tau_0$	(8.8 ± 17.4) yr	(27.7 ± 20.5) yr
Δv_0	(9.0 ± 5.6) km s^{-1}	(10.9 ± 5.8) km s^{-1}

The results of the least squares fits to the Δx vs. x_j and $(\Delta x)^2$ vs. x_j dependencies are shown in Figure 1. The coefficients of the (linear Δx vs. x_j and quadratic $(\Delta x)^2$ vs. x_j) fits, together with the errors estimated through the fitting procedure, are given in Table 1.

Proper motion measurements (see, e.g., Reipurth et al. 2002) indicate that the knots close to the source of the HH 34 system have plane of the sky velocities $v_j \approx 150$ km s^{-1}. Using this velocity and the parameters derived from the fits, from equations (4–6) we obtain the mean values of the widths of the ejection time (τ_0 and Δv_0) and of the ejection velocity (v_0 and Δv_0) distributions. The resulting values (together with their uncertainties) are given in Table 1.

3.4. *The HH 111 knots*

Noriega-Crespo et al. (2011) present a *Spitzer* image of the HH 111 system. This system does not show such a clearly symmetric structure as the HH 4 outflow. This fact is illustrated in Figure 2.

From the observed jet and counterjet structures, we choose a set of 5 well defined knot pairs which appear to have clear jet/counterjet correspondences (see Figure 2). We then use these 5 knot pairs to obtain the Δx vs. x_j and $(\Delta x)^2$ vs. x_j dependencies. The fits to these dependencies are shown in Figure 3, and the resulting coefficients are given in Table 1.

From the values of the coefficients from the fits and a $v_j \approx 240$ km s^{-1} plane of the sky velocity (see, e.g., Hartigan et al. 2001), we obtain the parameters of the ejection time and velocity distributions (τ_0, $\Delta\tau_0$ and v_0, Δv_0, respectively). These parameters are given in Table 1.